Presented at the 35th European PV Solar Energy Conference and Exhibition, 24-28 September 2018, Brussels, Belgium

INLINE CHARACTERIZATION OF DIAMOND WIRE SAWN MULTICRYSTALLINE SILICON WAFERS

J. Haunschild[1], N. Bergmann[1], T. Hammer[1], K. Krieg[1], T. Kaden[1], O. Anspach[2], H. Schremmer[3], S. Rein[1]
[1] Fraunhofer Institute for Solar Energy Systems ISE, Heidenhofstraße 2, 79110 Freiburg, Germany
[2] PV Crystalox Solar Silicon GmbH, Gustav-Tauschek-Straße 2, 99099 Erfurt, Germany
[3] Hennecke Systems GmbH, Aachener Straße 100, 53909 Zülpich / Germany
Corresponding author: Jonas Haunschild | Phone: +49 (0)761 4588 5634 | e-mail: jonas.haunschild@ise.fhg.de

ABSTRACT: While for monocrystalline silicon ingot slicing diamond wire sawing processes are widely used, the general approach for slicing multicrystalline bricks has been based on slurry wire processes. Driven by a strong decrease in wafer prices recently, wafer manufacturers of multicrystalline materials switched rather quickly to the diamond-cut process, although several severe technological challenges were to be faced. Unfortunately, sawing is more difficult and an adaptation of solar cell production is essential for texturing processes considering diamond-cut wafer surface morphology. Also characterization methodologies must be adapted to these new material properties. Especially saw mark inspection and thickness topology measurements are key aspects of developments. General imaging methods also need to be evaluated for defect detection and wafer rating purpose. In this paper, an overview of inline characterization methods and their applicability on diamond-cut wafers will be given. Five out of eight methods need hardware or software adjustments to work on diamond-cut wafers. Special attention is paid to the photoluminescence analysis which allows a forecast of solar cell parameters if the relevant defect features are correctly extracted from the images. Due to the increased optical artifacts, this is not a trivial task.

Keywords: characterization, multicrystalline silicon, wire sawing, diamond wire

1 INTRODUCTION

The multicrystalline silicon (mc-Si) wafering market has rapidly turned from slurry cut to diamond-wire slicing processes. Respecting the rising cost pressure, the diamond cut process for multicrystalline wafers seems to prevail through its many benefits (especially the shorter sawing time) [1] and has become the next-generation slicing technique [2]. Especially in recent months, the prices for monocrystalline wafers have decreased a lot and were almost on the same level as for multicrystalline wafers. As the material quality of multicrystalline wafers is lower than of monocrystalline wafers, the manufacturing costs must be cheaper and thus the introduction of the diamond-cut technology on multicrystalline wafers is a pressing concern. However, still much research and development is necessary, as the slicing of multicrystalline wafers is more difficult than for monocrystalline wafers. Also, established texturing processes have reduced efficiency on the diamond-cut surface and the impact on solar cell efficiency is under investigation [3, 4].

But also inline metrology [5] needs to be adapted and therefore, in this paper, we will focus on the challenges which metrology faces when dealing with the diamond-cut surface on multicrystalline wafers. After summarizing the technological differences between slurry cutting and diamond cutting, we give an overview of state-of-the-art characterization techniques and of the common parameters which are addressed during inline inspection. Then, we discuss why those inspection methods have limits on the diamond-cut surface, which sawing-issues are problematic and where further development is necessary.

2 THE WIRE-SAWING PROCESS

The common standard for wafer manufacturing is to use a wire saw to cut the monocrystalline ingot or the multicrystalline brick into wafers [6]. The wire is spooled around wire guides forming a wire web, so that the whole brick is cut at once when pushed through the running wire web. An illustration can be seen in Figure 1.

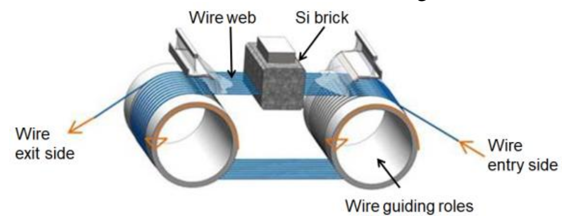

Figure 1: Scheme of the wire-sawing process.

The technological progress has brought various improvements to reduce the cutting time and increase overall quality and performance [7]. One of these improvements is the utilization of structured wire [8].

In recent years, many manufacturers have switched from plain-steel wires to wires coated with diamonds. When using the plain-steel wire, the cutting is done by small silicon carbide (SiC) particles, which are part of the cooling liquid called slurry. As the cutting performance is limited by the SiC particles, the time to cut a brick lies in-between 4-6 hours. With the introduction of the diamond wire process, the slurry can be replaced by a water based coolant. The cutting now is caused by fixed diamonds coated onto the wire. Obviously, the diamond wire is more expensive and therefore a bidirectional movement of the wire is applied with the wire being moved in forward direction and then moved back for a certain distance. This mode is called the pilgrim mode and reduces the usage of wire. Due to the better cutting efficiency of the coated diamonds compared to the SiC particles in the slurry, process time can be reduced down to 90 minutes for a monocrystalline ingot and a wire speed up to 33 m/sec [9]. For multicrystalline bricks, 2-3 hours are needed. Whether the cause for the reduced cutting efficiency lies in the presence of hard particles (SiN, SiC), different fracture strength of the grains or

other multicrystalline properties, is still under investigation [10–12].

One important aspect from a metrologist´s view is illustrated in Figure 2. While the brick is pushed through the wire web, the web is bent. In slurry cutting, this shape is also present, but hardly recognizable after the process. For diamond cutting with pilgrim mode being applied, we observe strong concave shaped variations of reflection and thickness on the wafers. These inhomogeneities are a challenge for inline wafer metrology, as will be pointed out in section 4 of this paper.

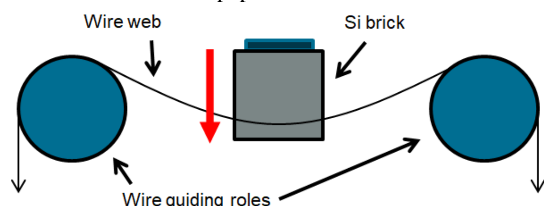

Figure 2: Side view illustration of the wire sawing process. The mc-Si brick is pushed through the wire web with constant speed. The pilgrim mode in the diamond-cut process thus forms concave-shaped marks on the wafers.

According to ITRPV, monocrystalline cutting is almost done exclusively with the diamond-wire process. For multi the situation is different. Not only is the diamond-cut process on multi more challenging than on mono, also the texture process in the beginning of the cell manufacturing process faces a technological challenge. For monocrystalline wafers, an alkaline etching solution is used forming a lowly reflecting pyramidal structure. The alkaline texture works fine with the rough surface from slurry cutting and the smooth surface from diamond cutting, especially as a saw-damage etching is applied beforehand. Unfortunately, the alkaline texture is not applicable on multi because of its varying grain orientations. The standard acidic texturing process needs a rough surface and performs poorly on the smooth surface of diamond-cut wafers. Both technological challenges have prevented the multicrystalline wafer manufacturing process from switching quickly to diamond cutting so far.

However, recent improvements and cost reductions in the monocrystalline wafer manufacturing have led to a significant decrease of wafer prices. According to our metrology partners, almost all multicrystalline production lines have switched from slurry cutting to diamond cutting in order to stay competitive. This sudden change seems to come along with non-optimal sawing conditions.

3 INLINE WAFER INSPECTION

3.1 Checking the specification

During incoming inspection for solar cell processing or outgoing inspection of wafer manufacturing, inline wafer inspection systems are used. The main purpose is to check the specifications of the wafers, to sort out wafers which do not meet the specifications, or to do a quality binning. The specifications cover different aspects and can be divided into surface, geometry, electric and material properties:

- Surface properties: stains, saw marks, chips, etc.
- Geometric properties: size, angels, thickness, total thickness variation (TTV), cracks, etc.
- Electric properties: resistivity, doping, lifetime, etc.
- Material properties: structural defects, crystallinity, oxygen, iron, inclusions, etc.

Not all of them are inline accessible. For example, there is no method up to now to measure oxygen, iron or other elemental concentrations inline within the wafers. Unfortunately, these impurities are decisive for a variety of meta-stable defects or degradation behavior. The charge carrier lifetime is a special case. While there are several inline methods to measure this parameter, it is limited in the as-cut state by surface recombination and thus holds little information on bulk recombination. Ways to overcome this limitation are to rate structural defects like dislocations or to calculate the bulk lifetime with a surface model. This topic will be covered in section 4.2.

3.1 Inline wafer inspection systems

In this work, the inline characterization tool HE-WI-06 from Hennecke Systems [13] has been used. Comparable machines are available from Semilab [14], Applied Materials [15] and others. Eight characterization modules are available in our HE-WI-06: (1) Thickness, (2) Resistivity, (3) Saw Marks, (4) Stain, (5) Micro Cracks (IR Transmission and Transflection), (6) Edge, (7) Geometry and (8) PL. These modules, their measurement types and the underlying SEMI standards [16] are depicted in Table 1.

Table I: Overview of the inspection modules of the Hennecke HE-WI-06 wafer inspection system and the related SEMI standards.

Module	Type	Standard
1) Thickness	capacitive *3 lines*	PV41
2) Resistivity	inductive *middle line*	PV28
3) Saw Marks	optical *laser line topology*	PV40
4) Stain	optical *diffuse illumination*	none
5) Micro Cracks	optical *IR transmission*	PV39
6) Edge	optical	none
7) Geometry	optical	PV46
8) PL	optical *IR luminescence*	PV51

It is important to note that all optical inspection modules needed an adjustment in terms of optical design, to work with the shiny diamond-cut surface. Existing inspections lines can be upgraded to be appropriate for the diamond-cut surface.

3.2 Sample set

A broad analysis of inline measurement methods applicable to diamond-cut as-cut wafers was carried out to investigate diversifying slicing effects. To learn from as many effects as possible, a large sample set of 2400 wafers was provided by PV Crystalox including 36 process variations on varying ingot materials [12]. Additional 1600 wafers with high quality from five different suppliers are part of the sample set. For comparison also wafers from a wafer set of 13000 slurry-cut wafers for production are taken into account.

All wafers have been thoroughly characterized and selected samples were textured to learn which surface issues remain visible after texturing.

4 RESULTS

4.1 Common issues

Before we deal with defects which are specific for mc-Si diamond-cut wafers, we will give some brief but important examples for incoming wafer inspection in general. The parameters to be addressed are listed in section 3.1 and the inspection modules are listed in table 1. In Figure 3, two examples are shown, a) microcrack detection and b) stain detection. A reliable detection and sorting out of (micro)cracks is very important, as cracked wafers can break in a later processing stage and cause machine downtime. Fortunately, the detection methods have improved a lot in the past years [17]. In infrared transmission images cracks are visible, but also grains and grain boundaries form similar strong contrasts. Thus, the detection rate is limited to avoid false positives. An improvement is the infrared transflection method, where the light source is on the same side as the camera. In this setup, the cracks act as scatter centers and reflected the light into the camera. Signatures of cracks with a higher contrast are the result. The downside is that in this setup, inclusions of particles cannot be detected anymore, so that both systems are part of the standard inspection modules of the HE-WI-06. In Figure 3a, an infrared transflection image is shown with a crack having a very distinct contrast and being easily detectable with inline image evaluation. In Figure 3b, an image of another module is shown. Here, a diffuse white light illumination is used to filter out reflection inhomogeneities and to find residuals from cleaning, handling or packaging. Depending on the follow-up processes, such stains need to be avoided and affected wafer to be sorted out.

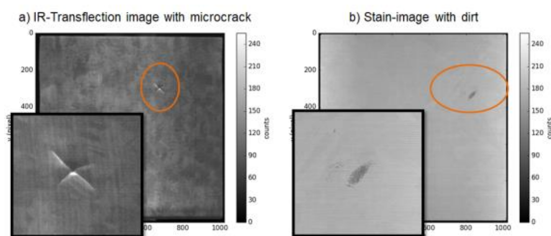

Figure 3: Common issues during incoming inspection of mono and multicrystalline wafers are the detection of (a) cracks and (b) stains. The images show diamond-cut wafers and for this surface the optics of the systems had to be adjusted to yield proper results.

4.2 Dislocations and impurities

One very important issue with multicrystalline wafers are structural defects. Grain boundaries and dislocations can be highly recombination-active and can significantly reduce efficiency of solar cells [18–20]. Also increased impurity concentrations in top- and bottom regions of bricks and edge regions of ingots can have a similar negative influence on efficiency. Both can be observed in PL images and the suppliers of wafer inspection system offer appropriate solutions.

In Figure 4, four Photoluminescence-Images (PL) are shown with different amounts of dislocations. Rating and highlighting here comes from the Hennecke PL-rating algorithm [21]. The given efficiency values are from the same wafers being processed to PERC solar cells. In this case, we observe $1.7\%_{abs}$ efficiency loss due to dislocations. Such a big impact of this material property can easily cover intentional process variations and thus needs to be monitored. Also, we recommend to perform a sorting of the wafers into different quality bins or sort out all wafers above a certain dislocation level. For the algorithm to work properly, we need a homogenous surface. Within the next section, we will discuss some examples where this condition is not fulfilled and will cause errors.

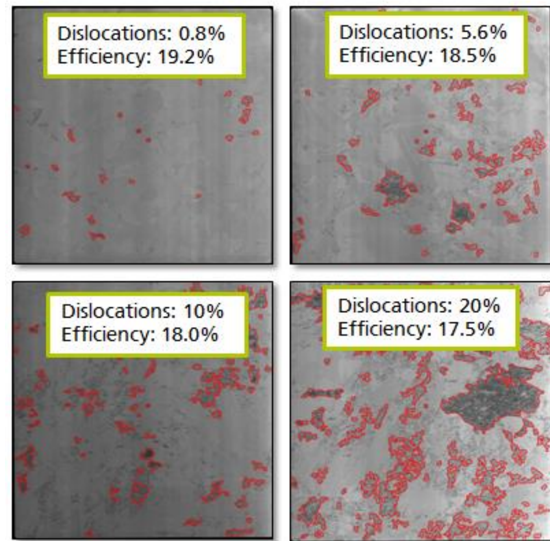

Figure 4: Four PL-Images of wafers with different dislocation (marked in red) values. Underneath the dislocation value, the efficiency of the solar cells is shown, which were made from these wafers.

One important note on this topic is that the manufacturers of PL-Systems follow different approaches and have different metrics for rating the images [20–23]. These metrics are based on a combination of image features, such as dislocations and impurities. For a more accurate rating, more image features like intensities, lines, patterns or even abstract filter responses are taken into account. While a rating for low-level Al-BSF solar cell processes can follow an analytic combination of the most common features, we observe that solar cell processes with high lifetime potential (e.g. PERC) require additional information from incoming inspection and a training of the rating model [20].

Other approaches to get information on the electrical material quality are: (i) The actual bulk lifetime can be calculated from the effective lifetime, which can be measured in as-cut state. A surface recombination model has to be taken into account for this approach [24, 25]. (ii) The effective lifetime can already be measured on brick level yielding significantly higher values due to lower surface recombination [26, 27]. (iii) A third approach is to apply a temporal wet chemical passivation (e.g. during texturing) to reduce the surface recombination velocity. In this case, the metrology tool needs to be placed within the wet chemical environment [28, 29].

4.3 Total thickness variation

After we covered some common issues and the topic of PL-Imaging, we now move to a basic wafer characteristic, which seems to be trivial, but needs to be handled with care on diamond-cut surface.

The total thickness variation (TTV) is calculated by the maximum value minus the minimum value. The

characterization module used for this is the E&H MX152. It generates three line scans by means of capacitive sensors. Each scan gathers 500 data points over a whole 156x156 mm^2 wafer depending on the belt speed. In Figure 5, we see a visualization of the three traces for a slurry-cut wafer (a) and a diamond-cut wafer (b). The slurry-cut wafer shows its typical wedge-like structure with lower values at the upper side of the image. The cause for this structure is that the silicon carbide particles in the slurry reduce in size during the sawing process and thus the wafer thickness changes. The diamond-cut example features typical traces of saw marks, which not only cause a reflectivity variation from the pilgrim mode, but also a more inhomogeneous topology.

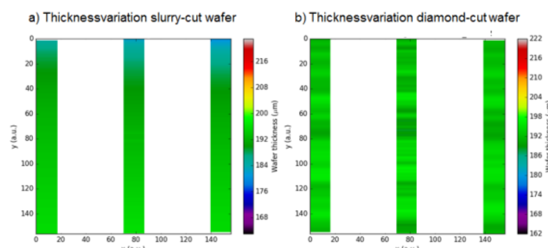

Figure 5: Visualization of the three-line measurement with capacitive thickness sensors. (a) The slurry-cut example features a smooth, but wedge-like surface. (b) The diamond-cut wafer shows a varying thickness due to saw marks.

In order to get a better impression of common TTV values, we analysed two datasets from the PVTEC laboratory. The first one contains 13,000 high-quality mc-Si wafers. This dataset (see Figure 6a) has TTV values roughly between 5-20 µm. In Figure 6b, a dataset of diamond-cut wafers is displayed and the colored histograms show different manufacturers. It has to be taken into account, that these also contain experimental wafers with sawing variations. So, we observe a bigger scattering but also lower TTV values. With technological improvements, we expect the TTV on diamond-cut mc-Si wafers to reach mean values well below 10µm.

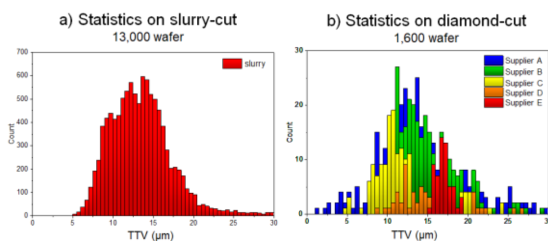

Figure 6: Histograms of a slurry-cut data set (a) and a diamond-cut wafer set (b). The histogram of total thickness variation of the slurry-cut wafers has its maximum between 10-20µm because of the wedge-like structure. The diamond-cut dataset is more experimental and this shows more variation. Five manufacturers are highlighted to show specific differences in TTV.

As pointed out in the beginning of this section, there is one very important point when measuring diamond-cut wafers. If the measurement traces are in line with saw marks, most of the wafers topology cannot be measured. Only if the measurement traces are perpendicular to the saw marks, the thickness variations can be covered. In Figure 7, this behavior is shown. Graph a) shows the histogram of a wafer box with 200 wafers which was measured in standard orientation (0°, with saw marks perpendicular to the direction of travel in the wafer inspection system) in blue and the measurement of the same wafers rotated by 90° with the saw marks then being parallel to the direction of travel in red. We observe the expected result for slurry-cut wafers: the histograms overlap. With diamond-cut wafers this is not the case. In Figure 7b, we see a strong deviation of the two histograms, the one measured in parallel to the direction of travel showing very low values. The origin of these low values is that only few saw marks are covered.

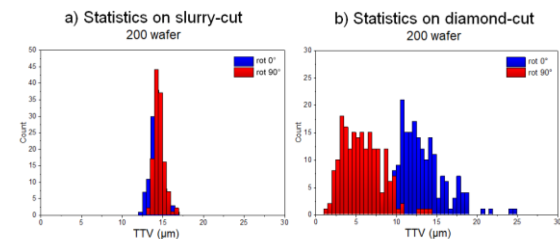

Figure 7: Histograms of a sample box with 200 slurry-cut wafers (a) and diamond-cut wafers (b) for a measurement parallel (red) and perpendicular (blue) to the saw marks. Due to the rather smooth surface of the slurry-cut process, the result is independent of the measurement direction. For the diamond-cut wafers, the measurement direction plays a decisive role.

As a consequence, the TTV of diamond-cut wafers (mono and multi) can only be measured accurately, if the wafers are measured with the correct orientation. Unfortunately, some wafer sawing- and sorting systems cannot maintain the rotation of the wafers and thus wafer stacks can be differently rotated in the wafer boxes.

4.4 Sawing issues

In the following, we discuss three examples of different surface conditions arising from different parameter setting of the cutting process or process problems.

a) Different sawing speed

As pointed out in the beginning, an increased speed (table or wire speed) in sawing will directly improve productivity and thus lower the costs. Typically, the pilgrim rate is kept at a constant level, so that by a faster pushing of the brick through the wire web, fewer pilgrim waves should be noticeable on the wafer and the reflection should be lower. This behavior can be seen in Figure 8. In this comparison of two typical diamond-cut mc-Si wafers, we observe that the pilgrim waves are clearly visible in the optical images, with 130 pilgrim waves on wafer A and 200 pilgrim waves on wafer B. The total reflection at 600 nm was measured offline with values of 31.7% and 33.5%, respectively. Such differences are no challenge for the metrology tools.

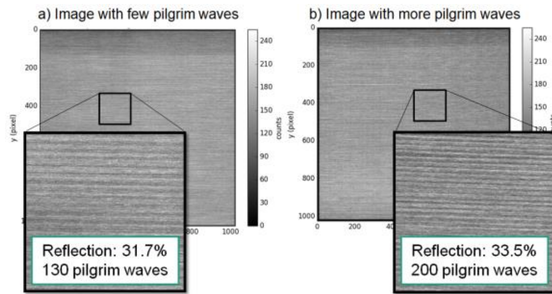

Figure 8: A comparison of two diamond-cut mc-Si wafers from optical inline inspection. The pilgrim waves are visible and influence the reflection value.

It is interesting to note that the multicrystalline grain structure is not visible in Figure 8. The cause is the higher proportion of direct reflection from these wafers. Visualizing the grain structure through the saw marks is rather difficult. This can be problematic if the grain structure needs to monitored, e.g. for quasi-mono wafers. After texturizing the wafers, the grain structure becomes visible, but the saw marks remain and the reflection is too high for solar cells with highest efficiencies. This can be observed in Figure 9. As pointed out in the beginning, better or improved versions of the acidic texture are needed.

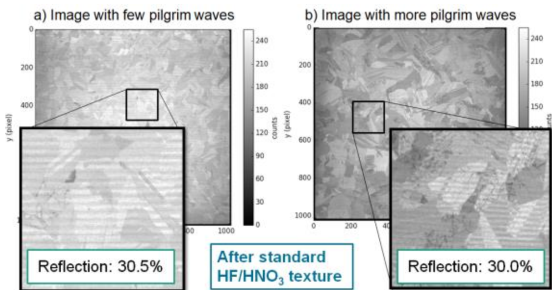

Figure 9: After texturizing the wafers from Figure 8, the grain structure becomes visible, while the pilgrim waves are still present. The lower reflection is not sufficient for making good solar cells.

b) Variation in sawing speed

In the second example, we encounter a more challenging artifact. Many wafers feature a more or a less reflecting part then the rest of the wafer´s surface. The reason lies in the sawing process. Before the sawing process is finished, the pushing speed is reduced in order not to cut too deeply into the connection of the brick to the sawing machine. This leads to a more polished surface in this region. This feature is common for mono- and multicrystalline diamond-cut processes and can be more or less pronounced.

In Figure 10, we find the optical image of a wafer with strongly increased reflection at the bottom edge of the wafer. In the image, the higher reflecting part has a lower count rate. This change in contrast can cause problems for the automatic detection algorithms for surface defects (e.g. stains, chips, cracks, etc.).

After texture, we again can clearly observe the grains and saw marks. In addition we observe the region to be more reflecting which might cause a power loss on solar cell level or form an undesired pattern on module level.

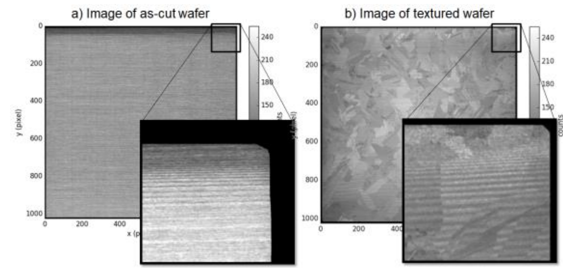

Figure 10: (a) A typical finding are wafers with a different reflectivity at one side. (b) After texturing the difference in reflectivity is reduced and grains and saw marks become visible.

c) Step contrast

The third example of surface artifacts causes very strong contrast at an arbitrary position on the wafers, being clearly visible also with the naked eye. Two examples are shown in Figure 11. The reason for this step-like contrast can have several origins, which cannot be distinguished from only the images. It can be a general problem with the sawing machine (wire rapture, coolant problem), a very rapid change in sawing speed (similar to the previous example), or it can be a silicon carbide particle forcing the sawing wire to shift. As previously stated, this strong contrast causes problems in the image evaluation (especially stain and PL). An example for false detection is given in Figure 12. After texture, the contrast remains visible (Figure 13).

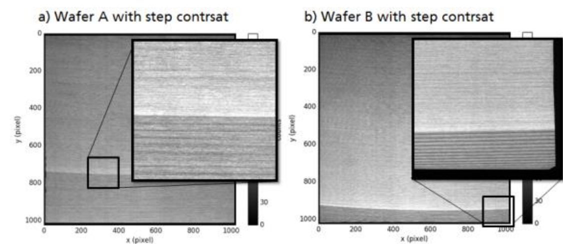

Figure 11: A very strong change in reflectivity on the wafer can lead to problems in the image evaluation. Such features remain visible after texture.

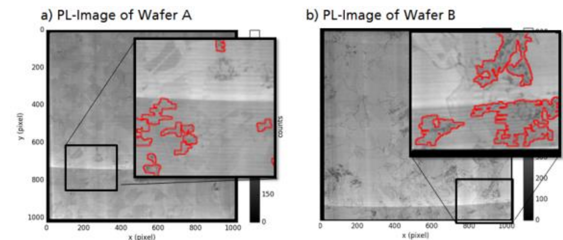

Figure 12: PL-Images of these wafers. The step contrast leads to a false detection of dislocations.

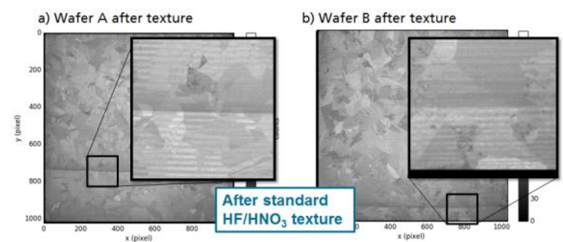

Figure 13: Visual images of these wafers after texture. The step contrast remains visible.

As a final remark, we can state that differences in reflectivity are a problem not only for texturing but also for inline metrology. For best error recognition results, the inspection modules and the image evaluation algorithms are optimized for a certain reflection. If the reflectivity changes (due to different sawing conditions), the accuracy in finding defects is reduced and by that false detections are more likely. Especially when the surface of the wafer is inhomogeneous (examples b and c), the detection of defects is challenging. For the algorithms to be fast enough with inline speed while dealing with high resolution, they need to be simple. Rather than time-consuming contrast-invariant methods, simple thresholding or grey-scale contrast algorithms are applied. If now, the reflectivity and thus the grey-values of the camera signal are changing, then errors in image evaluation can be the consequence.

The manufacturers of the inline inspection systems are working on that problem. One approach is to measure the reflectivity of the wafers and pass the result to the cameras in order to set the optimal visual conditions for image processing. However, if there is a sudden change of reflectivity on the wafer, this approach will not work.

5 CONCLUSION

In this work, we analysed the status of inline metrology when dealing with diamond-cut surfaces in general und multicrystalline wafers in special. Most visual inspection systems had to undergo a hardware modification in order to measure on the more reflecting diamond-cut surface. We observe that the common issues that need to be checked for wafer specification (e.g. size, thickness, cracks, doping, etc.) can be accessed with high accuracy. Differences or problems in the sawing process can cause strong inhomogeneities and variations in reflection on the wafer surface, which disturb the imaging methods and can cause problems in the detection algorithms.

For multicrystalline wafers, the detection of PL-features such as dislocations and impurities is of major importance, because these parameters allow a rating of the electric quality in terms of IV parameters. The existing metrics from PL manufacturers are not comparable. Regarding the measurement of wafer thickness and the total thickness variation, we observe that the direction of measurement has to be taken into account, because saw marks parallel to the measurement direction cannot be detected.

Further work has to be invested in order to increase the quality of the diamond-cut surface, while inline metrology has to develop better algorithms and to be able to work with wafers which have a partially different reflecting structure.

7 AKNOWLEGMENTS

This work was funded by the German Federal Ministry for Economic Affairs and Energy within the project “DIADEM” (contract number 0324091B).

8 REFERENCES

[1] A. Bidiville, K. Wasmer, R. Kraft, and C. Ballif, “Diamond Wire-Sawn Silicon Wafers – from the Lab to the Cell Production,” (eng), 2009.

[2] F. Cao *et al.,* “Next-generation multi-crystalline silicon solar cells: Diamond-wire sawing, nano-texture and high efficiency,” *Solar Energy Materials and Solar Cells*, vol. 141, pp. 132–138, 2015.

[3] H. Seigneur, E. J. Schneller, N. S. Shiradkar, and W. V. Schoenfeld, “Effect of Diamond Wire Saw Marks on Solar Cell Performance,” *Energy Procedia*, vol. 92, pp. 386–391, 2016.

[4] e. a. B. Kafle, “On the fabrication of high-efficiency mc-Si PERC-based solar cells on diamond wire-sawn surfaces using industrially viable etching technologies,” *PV International*.

[5] J. M. Greulich *et al.,* “In-line quality control in high efficiency silicon solar cell production,” *Photovoltaics International*, vol. 35, pp. 46–57, 2017.

[6] H.J. Möller, “Basic Mechanisms and Models of Multi-Wire Sawing,” *advanced engineering materials*, vol. 2004.

[7] A. Kumar and S. N. Melkote, “Diamond Wire Sawing of Solar Silicon Wafers: A Sustainable Manufacturing Alternative to Loose Abrasive Slurry Sawing,” *Procedia Manufacturing*, no. 21, 2018.

[8] O. Anspach, B. Hurka, and K. Sunder, “Structured wire: From single wire experiments to multi-crystalline silicon wafer mass production,” *Solar Energy Materials and Solar Cells*, vol. 131, pp. 58–63, 2014.

[9] Meyer Burger, *Factsheet DW 291*.

[10] C. Yang, H. Wu, S. Melkote, and S. Danyluk, “Comparative Analysis of Fracture Strength of Slurry and Diamond Wire Sawn Multicrystalline Silicon Solar Wafers,” *Adv. Eng. Mater.*, vol. 15, no. 5, pp. 358–365, 2013.

[11] T. Kaden, “Optimization potential of the wire sawing process for multicrystalline silicon,” *Photovoltaic International*, vol. 37, 2017.

[12] K. Sunder, R. Buchwald and O. Anspach, “Origin of the periodic strucutre of diamond wire sawn wafers,” in *31th EUPVSEC*.

[13] MeyerBurger. [Online] Available: http://www.meyerburger.com/de/en/meyer-burger/products-and-systems/detail/wis-06/.

[14] Semilab. [Online] Available: http://www.semilab.hu/category/products/u-pcd-carrier-lifetime-wafers.

[15] Applied Materials. [Online] Available: http://www.appliedmaterials.com/products/applied-vericell-solar-wafer-inspection-system.

[16] SEMI Standards for PV. [Online] Available: http://www.semi.org/en/industries/SolarPV.

[17] M. Demant *et al.,* “Microcracks in Silicon Wafers I: Inline Detection and Implications of Crack Morphology on Wafer Strength,” *IEEE J. Photovoltaics*, vol. 6, no. 1, pp. 126–135, 2016.

[18] J. Haunschild *et al.,* “Quality control of as-cut multicrystalline silicon wafers using photoluminescence imaging for solar cell production,” *Sol. Energy Mater. Sol. Cells*, vol. 94, no. 12, pp. 2007–2012, 2010.

[19] M. Demant, J. Greulich, M. Glatthaar, J. Haunschild, and S. Rein, “Modelling of physically relevant features in photoluminescence images,” *Energy Procedia*, vol. 27, pp. 247–252, 2012.

[20] M. Demant *et al.,* “Inline quality rating of multi-crystalline wafers based on photoluminescence images,” *Prog. Photovolt: Res. Appl.*, vol. 24, no. 12, pp. 1533–1546, 2016.

[21] H. Schremmer, A. Bergmann, J. Grohs, and N. Cüppers, “Precise cell performance estimation based on wafer PL measurement,” in *31st EU PVSEC*, Hamburg, 2015.

[22] F. Korsós, Z. Kiss, Ch. Defranoux, S. Gaillard, “Inline PL Imaging Techniques for Crystalline Silicon Cell Production,” Marseille, 2016.

[23] BT Imaging. [Online] Available: https://www.btimaging.com/products-c1g2d.

[24] K. Bothe, R. Krain, R. Falster, and R. Sinton, “Determination of the bulk lifetime of bare multicrystalline silicon wafers,” *Prog. Photovolt: Res. Appl.*, vol. 18, no. 3, pp. 204–208, 2010.

[25] R. A. Sinton, J. Haunschild, M. Demant, and S. Rein, “Comparing lifetime and photoluminescence imaging pattern recognition methodologies for predicting solar cell results based on as-cut wafer properties,” *Prog. Photovolt: Res. Appl.*, n/a, 2012.

[26] e. a. B. Mitchell, “PERC Solar Cell Performance Predictions From Multicrystalline Silicon Ingot Metrology Data,” *IEEE JPV*, vol. 7, 2017.

[27] N. Schüler, B. Berger, K. Dornich, and J. R. Niklas, “High resolution inline topography of iron in P-doped multicrystalline bricks by MDP,” *Energy Procedia*, no. 38, pp. 176–182, 2013.

[28] S. Al-Hajjawi, J. Haunschild, M. Zimmer, T. Dannenberg, R. Preu, “Predicting bulk lifetime values by applying wet Predicting bulk lifetime values by applying chemistry H-termination for inline quality control of silicon wafers,” in *Silicon PV 2017*.

[29] H. Sugimoto and M. Tajima, “Photoluminescence Imaging of Multicrystalline Si Wafers during HF Etching,,” *Jpn. J. Appl. Phys*, vol. 46, 2007.